Conformational plasticity of phospholipid headgroups in simulations and experiments

Amélie Bacle,[1] Pavel Buslaev,[2,3] Rebeca García Fandiño,[4,5] Fernando Favela-Rosales,[6] Tiago M. Ferreira,[7] Patrick F.J. Fuchs,[8,9] Ivan Gushchin,[3] Matti Javanainen,[10] Anne M. Kiirikki,[11] Jesper J. Madsen,[12,13] Josef Melcr,[10,14] Paula Milán Rodríguez,[8] Markus S. Miettinen,[15] O. H. Samuli Ollila,[11,*] Chris G. Papadopoulos,[16] Antonio Peón,[5] Thomas J. Piggot,[17] Ángel Piñeiro,[18] and Salla I. Virtanen[11]

[1]*Laboratoire Coopératif "Lipotoxicity and Channelopathies - ConicMeds", Université de Poitiers, 1 rue Georges Bonnet, 86000 Poitiers, France*
[2]*Nanoscience Center and Department of Chemistry, University of Jyvskyl, P.O. Box 35, 40014 Jyvskyl, Finland*
[3]*Research Center for Molecular Mechanisms of Aging and Age-related Diseases, Moscow Institute of Physics and Technology, 141701 Dolgoprudny, Russia*
[4]*Center for Research in Biological Chemistry and Molecular Materials (CiQUS), Universidade de Santiago de Compostela, E-15782 Santiago de Compostela, Spain*
[5]*CIQUP, Centro de Investigao em Química, Departamento de Química e Bioquímica, Faculdade de Ciências, Universidade do Porto, Porto, Portugal*
[6]*Departamento de Ciencias Básicas, Tecnológico Nacional de México - ITS Zacatecas Occidente, México*
[7]*NMR group - Institute for Physics, Martin Luther University Halle-Wittenberg, 06120 Halle (Saale), Germany*
[8]*Sorbonne Université, Ecole Normale Supérieure, PSL University, CNRS, Laboratoire des Biomolécules (LBM), 75005 Paris, France*
[9]*Université de Paris, UFR Sciences du Vivant, 75013, Paris, France*
[10]*Institute of Organic Chemistry and Biochemistry of the Czech Academy of Sciences, Flemingovo nám. 542/2, CZ-16610 Prague 6, Czech Republic*
[11]*Institute of Biotechnology, University of Helsinki*
[12]*Department of Chemistry, The University of Chicago, Chicago, Illinois, United States of America*
[13]*Global and Planetary Health, College of Public Health, University of South Florida, Tampa, Florida, United States of America*
[14]*Groningen Biomolecular Sciences and Biotechnology Institute and The Zernike Institute for Advanced Materials, University of Groningen, 9747 AG Groningen, The Netherlands*
[15]*Department of Theory and Bio-Systems, Max Planck Institute of Colloids and Interfaces, 14424 Potsdam, Germany*
[16]*Université Paris-Saclay, CEA, CNRS, Institute for Integrative Biology of the Cell (I2BC), 91198 Gif-sur-Yvette, France*
[17]*Chemistry, University of Southampton, Highfield, Southampton SO17 1BJ, United Kingdom*
[18]*Departamento de Física Aplicada, Facultade de Física, Universidade de Santiago de Compostela, E-15782 Santiago de Compostela, Spain*

(Dated: April 28, 2021)

Chemistry of lipid headgroups, the water facing components of cell membranes that regulate cell functions via lipid–protein interactions, varies between organisms and organelles. Because membranes are in liquid state under physiological conditions, individual lipids are not fixed to single conformations but they sample an ensemble of conformations with the Boltzmann weighted probabilities. However, these ensembles and their dependence on lipid types have not yet been experimentally determined. Therefore, it has not been clear if lipid molecules exchange between few rigid conformations, or if they can freely fluctuate in all possible conformations. Here, we combine solid state NMR experiments and molecular dynamics simulations from the NMRlipids open collaboration to resolve the conformational ensembles of the headgroups of key lipid types in their liquid lamellar phase under various biologically relevant conditions. Interpretation of NMR experiments using the plethora of simulation data collected in the NMRlipids project suggests that all lipid headgroups sample a wide range of conformations in neutral and charged cellular membranes. Differences in the headgroup chemistry between different lipid types manifest in probability distributions of conformations, but all lipid types can access almost any of the possible conformations. Together with the analysis of protein-bound lipids from the protein data bank (PDB), this suggests that lipids can bind to proteins in a wide range of conformations independently of their headgroup chemistry. Therefore, the selective adsorption of proteins to membranes is likely regulated by specific protein–lipid interactions rather than conformational restrictions of the bilayer lipids. Our results pave the way to comprehensive understanding of lipid mediated signaling and lipid–protein interactions in biomedical applications.

INTRODUCTION

Chemical compositions of hydrophilic lipid headgroups vary between different organelles and organisms, and different lipid types regulate protein functions in many different ways [1, 2]. Lipids can directly bind to proteins or indirectly affect protein functions by altering membrane properties such as charge or elasticity [1, 3]. Specific interactions with certain lipid headgroups are known to be essential for the function of several proteins [3, 4], but it is not clear if the specificity is driven by the differences in accessible conformations between lipid types or by specific lipid–protein interactions.

Stuctures of protein-bound lipids are available in the protein data bank (PDB) [5] and crystal structures of lipids have

been determined [6, 7], but their relation to the conformational ensembles in bulk membranes in the liquid lamellar phase remains unclear [8]. Most accurate experimental information on conformational ensembles of lipids in liquid lamellar phase are typically derived from NMR experiments, particularly from C–H bond order parameters measured using ^{2}H NMR [9–11]. According to these experiments, the glycerol backbone conformations are largely similar irrespectively of the headgroup [12] and the headgroup conformations are similar in phosphatidylcholine (PC), phosphatidylethanolamine (PE) and phosphatidylglycerol (PG) lipids, whereas the headgroup of phosphatidylserine (PS) lipids is more rigid [6, 13]. However, order parameter signs are not accessible in ^{2}H NMR experiments [14] and universal models to map order parameters to structural ensembles are not available [15, 16]. Therefore, it is not clear if the conformational ensemble of lipid headgroups in liquid lamellar bilayer is composed of exchange between few restricted conformations, or if lipid headgroups can fluctuate freely across a wide range of conformations.

Here, we use natural abundance ^{13}C NMR experiments and MD simulations from the NMRlipids open collaboration to resolve the differences in the conformational ensembles between PC, PE, PG and PS lipid headgroups. We elucidate also the effect of charges and protein binding to lipid headgroup conformations. Zwitterionic PC and PE are the most common lipids in eukaryotes and bacteria, respectively [2, 17]. PE is also the second most abundant glycerophospholipid in eukaryotic cells and has been related to various diseases [18–20]. PS and PG are the most common negatively charged lipids in eukaryotes and bacteria, respectively, and their presence affect membrane protein functionality and signaling [3, 17, 21, 22]. All the studied lipids specifically bind to various proteins [23].

Similarity of glycerol backbone and headgroup order parameters in model membranes and bacteria [12, 24, 25] suggest that our results can be used to understand the biological role of lipid headgroups in lipid–protein interactions. These interactions are crucial, for example, in lipid mediated signaling [3] and design of phoshoplipid-specific antibodies [26].

METHODS

Experimental C–H bond order parameters

The headgroup and glycerol backbone C–H bond order parameters of 1-palmitoyl-2-oleoyl-sn-glycero-3-phosphoethanolamine (POPE) and 1-palmitoyl-2-oleoyl-sn-glycero-3-phospho-(1'-rac-glycerol) (POPG), purchased from Avanti polar lipids, were measured using natural abundance ^{13}C solid state NMR spectroscopy as described previously [27, 28]. The magnitudes of order parameters were determined from the chemical-shift resolved dipolar splittings using a R-type Proton Detected Local Field (R-PDLF) experiment [29], and the signs from S-DROSS experiments [30] combined with SIMPSON simulations [31]. The NMR experiments were identical as in our previous work [32]. The POPE experiments were recorded at 310 K and POPG experiments at 298 K, where the bilayers are in the liquid disordered phase [33].

Glycerol backbone peaks from both lipids, and the α-carbon peak from POPE in the INEPT spectra were assigned based on previously measured POPC spectra [27]. The β-carbon peak from POPE was assigned based on ^{13}C chemical shift table for amines available at `https://www.chem.wisc.edu/areas/reich/nmr/c13-data/cdata.htm`. **1.How were α and γ-carbon peaks assigned in POPG?**. The β-carbon peak from POPG overlapped with the g_2 peak from glycerol backbone because their chemical environments are similar. **2.Details to be checked by Tiago.**

Molecular dynamics simulations

Molecular dynamics simulation data were collected and analyzed using the methods from the NMRlipids Open Collaboration project (`nmrlipids.blogspot.fi`) [14, 32, 34, 35]. Simulation details, accessibility information and quality evaluation of almost 100 combinations of lipid headgroup and force field simulated for this work are in the supplementary information.

Best models for the interpretation of lipid headgroup conformational ensembles from the experimental data were selected using quality evaluation measures defined in the NMRlipids project. Conformational ensembles of headgroup and glycerol backbone in PE and PG simulations were evaluated using the C–H bond order parameters [34]. Interactions between different headgroups were evaluated by monitoring the changes in headgroup order parameters upon mixing the lipids [32]. The ion binding affinities and response of lipids to bound charge were evaluated by monitoring the changes in lipid headgroup order parameters [32, 35].

The differences in headgroup conformation ensembles were analyzed calculating the distributions of the last six heavy atom dihedral angles, i.e., dihedrals O_α-C_α-C_β-N/C_γ, P-O_α-C_α-C_β, O_{g3}-P-O_α-C_α, g_3-O_{g3}-P-O_α, g_2-g_3-O_{g3}-P, and g_1-g_2-g_3-O_{g3} labeled in Fig. 1 C. Relative energy costs for turning dihedral angles with respect to the most probable value (lowest energy) were estimated from the inverse Boltzmann formula $\Delta E(\theta) = -kT\left[\ln\left[p(\theta)\right] - \ln\left[p(\theta_0)\right]\right]$, where $p(\theta)$ is the dihedral angle distribution and θ_0 is the most probable angle from MD simulation.

Analysis of protein-bound lipid conformations

Lipid structures from the Protein Data Bank (PDB, [38]) were searched using PDBe REST API (`www.ebi.ac.uk/pdbe/pdbe-rest-api`) using the ligand names listed in the supplementary information. Heavy atom dihedral distributions from the lipid structures were calculated using the

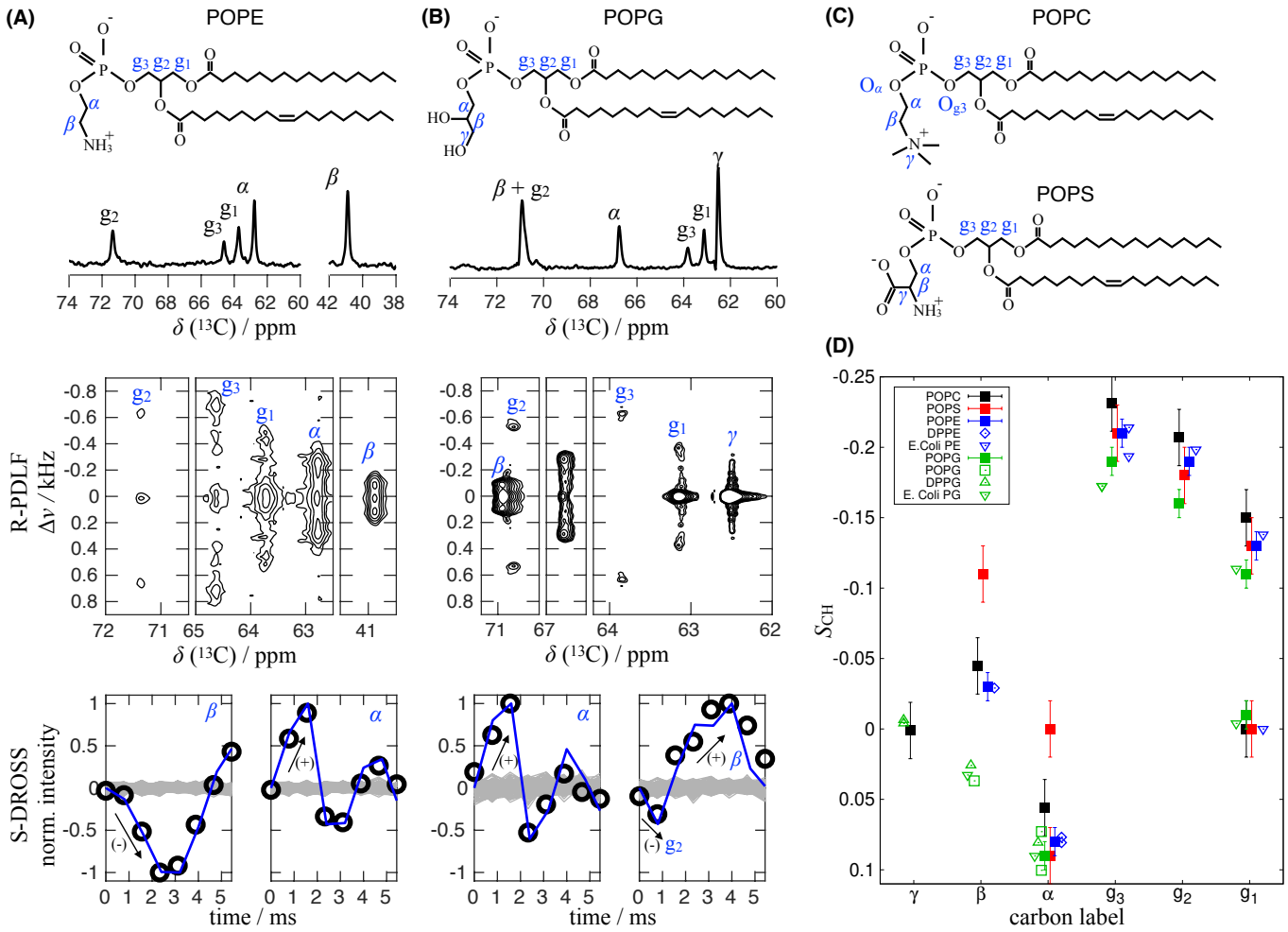

FIG. 1: Chemical structure, refocused-INEPT spectrum, 2D R-PDLF spectra, and S-DROSS dipolar slices (from top to bottom) for **A)** POPE and **B)** POPG MLVs measured by ^{1}H-^{13}C solid-state NMR. The S-DROSS dipolar slices show both experimental data (open circles) and the result of NMR numerical simulations (blue solid lines). Full NMR spectra are shown in Figs. S1 and S2. **C)** Chemical structure of POPC and POPS. **D)** Headgroup and glycerol backbone C-H bond order parameters for different phospholipids measured in the lamellar liquid disordered phase. The S_{CH} magnitudes and signs determined by ^{1}H-^{13}C NMR spectroscopy (filled squares) for POPE (310 K) and POPG (298 K) measured in this work are shown together with the data previously reported for POPS (298 K) [32] and POPC (300 K) [27, 28]. The headgroup and glycerol backbone S_{CH} magnitudes measured previously with ^{2}H NMR (empty symbols) are also plotted as real values using the signs determined in this work for POPG with 10nM PIPES (298 K) [36], DPPG with 10mM PIPES and 100mM NaCl (314 K) [13], DPPE (341 K) [37], E.coli PE and E.coli PG (310 K) [12] .

MDAnalysis Python library [39, 40] and Jupyter notebook available from *scripts/PDBanalysis.ipynb* folder in Ref 41. Only the structures determined using X-ray crystallography or Cryo-EM with a resolution higher than 3.2 Å were used in the analysis. Some structures of multimeric proteins contained multiple lipids in the same conformation (analyzed dihedral angles within 3 degrees of each other). In that case, this conformation was counted once for the subsequent analyses to avoid its overweighting.

To demonstrate the existence of similar structures of different lipids bound to different proteins, we searched for pairs having the last five headgroup heavy atom dihedral angles (excluding g_1-g_2-g_3-O_{g3}) within 30 degrees of each other among the structures with resolution higher than 2.5 Å. The two most representative examples were handpicked from the results.

RESULTS AND DISCUSSION

Differences between lipid headgroups from ^{13}C NMR experiments

To experimentally characterize the differences in headgroup conformational ensembles of lipids that are not bound to proteins, we measured the C–H bond order parameters and their signs of POPG and POPE in the liquid lamellar phase, as we did previously for POPC and POPS [27, 28, 32]. Determination of headgroup and glycerol backbone order parameters

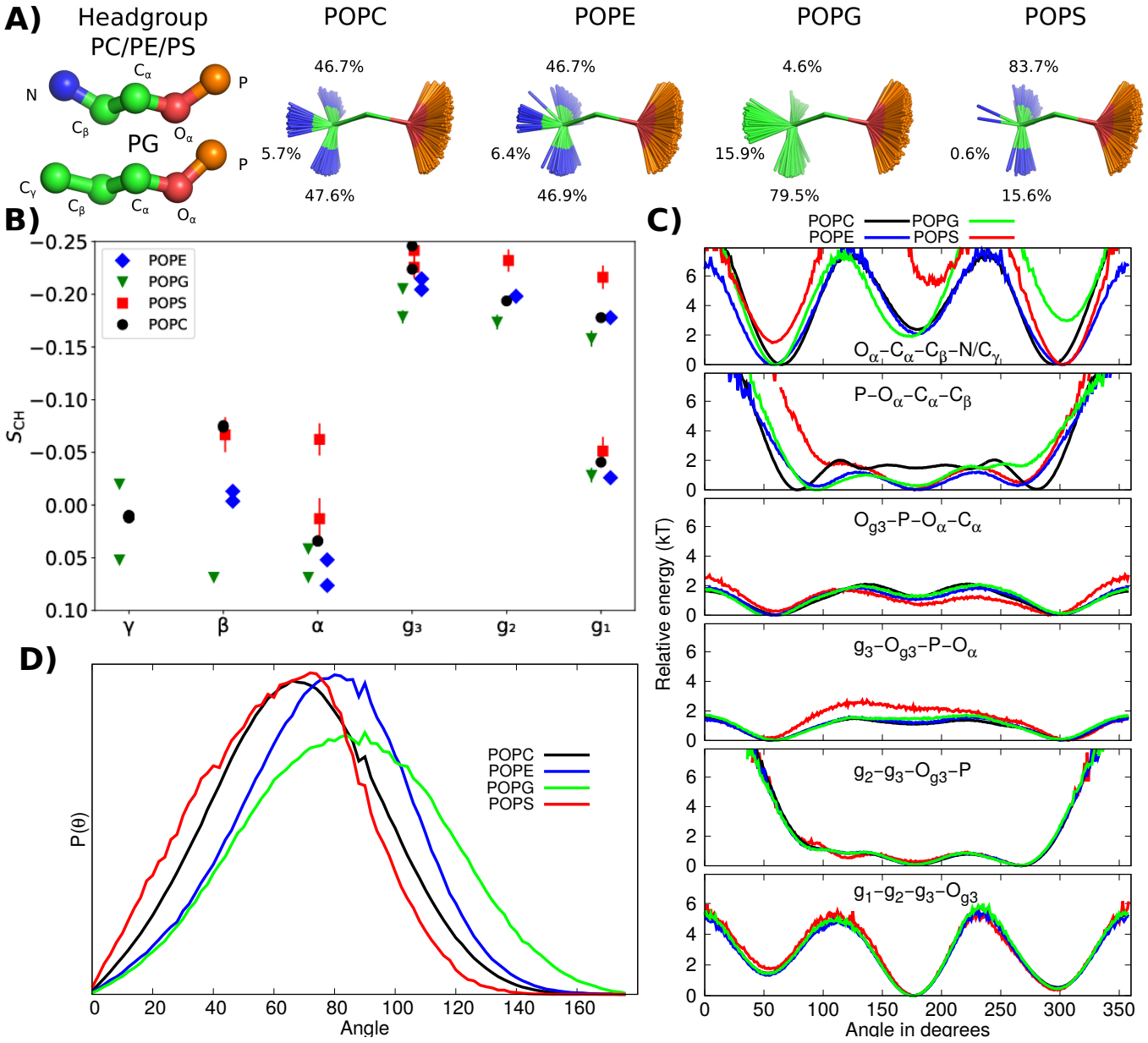

FIG. 2: Results from the best simulation model (CHARMM36) simulations demonstrating the differences in conformational ensembles between different lipids. **A)** Snapshots with overlayed C_β, C_α and O_α atoms and occurence of different conformations. **B)** Headgroup and glycerol backbone region order parameters of different different lipids. **C)** Relative free energies for individual heavy atom dihedral angles estimated from the inverse Boltzmann formula. Angles corresponding energies above 7 kBT are not shown because they are not observed in simulations. **D)** Distributions of P–N vector angle with respect to membrane normal.

and their signs was straightforward from the data in Figs. 1, S1 and S2 for all the C–H bonds, except for the β and g_2 carbons in POPG. These carbons have overlapping peaks in the INEPT spectra due to their similar chemical environments, and only the magnitude of the larger order parameter could be determined from the R-PDLF spectra (Fig. 1B). Based on previous ^{2}H NMR measurements [12, 13, 36], we assigned the larger order parameter to the g_2 carbon and used the literature value for the β-carbon in SIMPSON simulations to determine the signs. The decrease in the beginning of the S-DROSS curve suggests that the sign of larger g_2 order parameter is negative and later increase suggests that sign of smaller β order parameter is positive (Fig. 1B). This interpretation is confirmed by SIMPSON calculations in Fig. **??**.

Experimental order parameters of POPC, POPE, POPG and POPS glycerol backbones and headgroups from this and previous studies are collected in Fig. 1D, where the signs from ^{13}C NMR experiments are used also for the ^{2}H NMR data from the literature. The overall agreement of order parameters determined by different research teams and different tech-

niques for the same lipid headgroup is excellent here and in previous studies [14, 32, 34]. Therefore, the differences between lipid types are dictated by the headgroup chemistry rather than inaccuracies in experiments, differences in the acyl chains, or in experimental conditions.

The most distinct order parameters are observed for PS headgroups, for which the α-carbon order parameter exhibits significant forking (different values for different hydrogens bound to the same carbon) and the β-carbon has a more negative value than other studied lipid types. On the other hand, the β-carbon order parameter of PG headgroup has a positive sign, in contrast to all the other lipid types. This has not been previously observed in ^{2}H NMR experiments detecting only the absolute values [12, 13, 36]. The glycerol backbone order parameters are similar for all the lipid types, although they move slightly toward positive values (closer to zero) in the order PC $<$ PE $<$ PS $<$ PG. Only minor differences between PC and PE headgroups are observed.

Conformational ensembles of different lipid headgroups from MD simulations

MD simulations could be used to interpret the lipid conformational ensembles from experiments due to their direct connection to the measured C-H bond order parameters. To find the best models for this purpose, we took advantage of the power of the NMRlipids project which has gathered a massive number of trajectories using open collaboration. We have thereby evaluated all the available MD simulation force fields of PC [34], PS [32], PE (Fig. S3), and PG (Fig. S4) lipids against NMR data in the NMRlipids project. The comparison of hundreds of simulation trajectories simulated with approximately 20 different force fields reveal that none of the current parameters can correctly capture the lipid conformational ensemble and reproduce the experimental C-H bond order parameters of all segments. However, the best parameters (CHARMM36) correctly capture the essential differences between PC, PE, PG and PS headgroup order parameters (Fig. 2 B).

To understand the structural origin of distinct order parameters for PG and PS lipids, we first calculated the heavy atom dihedral angle distributions from the best performing simulations that reproduced the differences between headgroups (Fig. S11). Then, we used the inverse Boltzmann formula to estimate the energy costs for different dihedral angle orientations. The results in Fig. 2C suggest that all lipid headgroups are very flexible and energy costs for rotating individual dihedrals to almost any angle is low (below 7 $k_{\mathrm{B}}T$). Only cis states of P-O_α-C_α-C_β and g_2-g_3-O_{g_3}-P have larger relative energies and are not observed for any lipids during the simulations.

Major differences between headgroups are observed for the last two dihedrals in the headgroup end, O_α-C_α-C_β-N/C_γ and P-O_α-C_α-C_β, which prefer *gauche*$^-$ conformations for PG and *gauche*$^+$ for PS, whereas PC and PE exhibit symmetric distributions. Also, the energy barriers for O_α-C_α-C_β-N/C_γ dihedral rotations between *gauche* and *trans* states are larger for PS and PG lipids than for PC and PE lipids. Rest of the dihedrals are similar between different lipids, with the exception of PS lipids for which slightly larger energy for *eclipsed anti* conformation in g_3-O_{g3}-P-O_α dihedral was observed. Therefore we suggest that the main differences between lipid headgroups leading to distinct order parameters occur in the headgroup end, while phosphate region remains similar in different lipids with the exception of PS. The increased barriers for dihedral rotations may explain the more rigid headgroup structures in PS [6, 43]. Furthermore, the angle between headgroup dipole and membrane normal decreases in the order of PG $>$ PE $>$ PC $>$ PS (Fig. 2D). However, the differences between PC and PE in P-O_α-C_α-C_β dihedral and P–N vector dipole may be artificial as the β-carbon order parameter in PC is too negative even in the best available force field, thereby not being equal to the order parameter in PE as observed in experiments [34].

In conclusion, all studied lipid headgroups sample very broad conformational ensembles in the liquid lamellar phase and the sampled dihedral angles are within similar ranges for all headgroup types. Since the rotation of dihedral angles to almost any position bears relatively low free energy cost, the lipid headgroups are able to adopt a wide range of conformations when interacting with proteins, ions, or other biomolecules. Therefore, the structures in lipid crystals [6, 7] are not representative of the liquid state, and models aiming to explain NMR data using only a few conformations [9–11, 16] are not sufficient to capture the large conformational space of lipids in the liquid lamellar state. However, MD simulations with accurate force fields can be expected to capture the correct conformational ensembles of lipids.

Lipid conformational ensembles in charged membranes

Charged entities, such as lipids, proteins, surfactants, drugs, and ions incorporated in membranes can reorient the headgroup dipole in PC lipids and affect the order parameters of the lipid headgroups [44]. However, the detailed understanding of the structural and energetic responses of lipids to membrane-bound electric charge is still lacking [11].

To resolve lipid headgroup conformational ensembles in cellular membranes bearing positive charge, we calculated the heavy atom dihedral angle distributions from the subset of simulations that correctly captured the experimentally measured decrease in PC headgroup order parameters upon addition of cationic surfactants into a bilayer (figure 3 A). The dihedral angle distributions and relative energies in figures S12 and 3 B) reveal that the addition of positive charge into a membrane decreases the abundance of *trans* states in g_2-g_3-O_{g_3}-P and g_3-O_{g_3}-P-O_α dihedrals. The choline region remains essentially unchanged and only minor changes are observed in other dihedrals even at a surfactant molar fraction of 0.47.

In addition, binding of ions to the membrane may affect the

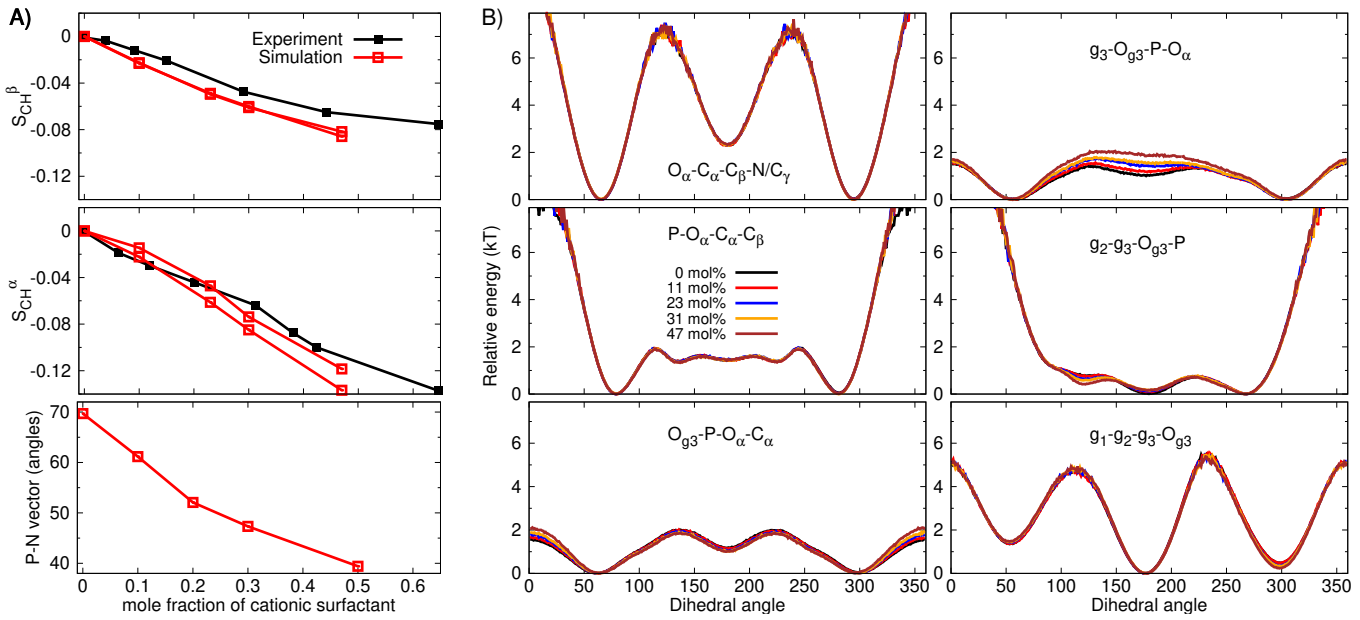

FIG. 3: **A)** Modulation of PC headgroup order parameters and P–N vector angle upon addition of cationic surfactant (dihexadecyldimethylammonium) from CHARMM36 simulations compared with the experimental data [42]. **B)** Relative energies for individual dihedral angles estimated from inverse Boltzmann distributions of heavy atom dihedral angles with different amounts of cationic surfactant from CHARMM36 simulations.

lipid headgroup conformational ensembles under physiological conditions. The bound Ca^{2+} ion to PC headgroup leads to similar decrease in trans state probability for g_3-O_{g3}-P-O_α dihedral in the most realistic MD simulation models as observed for cationic surfactants (lipid17ecc and CHARMM36 in Figs. S13, S14 and Fig. S7). The dihedral distributions of the PG headgroup are more sensitive to the bound ions in the most realistic simulations, but upward tilting of the headgroup dipole upon the addition of $CaCl_2$ is weaker than in PC (Lipid17 and Slipids in Figs. S7, S15 and S16). However, the changes in PG lipid dihedrals upon the addition of $CaCl_2$ differ between the best models (Figs. S15 and S16), and none of the simulations captures the Ca^{2+} ion binding affinity and conformational ensemble of PG lipids simultaneously. Moreover, experimental data to evaluate the response of α-carbon order parameters to the added $CaCl_2$ in PG is not available. Additionally, the headgroup conformational ensembles in mixtures of PC and charged (PG or PS) or zwitterionic (PE) lipids could not be resolved with the currently available force fields and experimental data (Figs. S5 and S6, and Ref. [32, 45]).

In conclusion, the structural response of lipid headgroups to membrane-bound charges arise from mild changes in dihedral angle distributions, rather than restriction of lipids to fixed conformations. Therefore, lipid headgroups sample a large space of different conformations also in charged membranes, thereby retaining the capability to adopt multiple conformations when interacting with proteins or other molecules.

Protein-bound lipid conformations

Interpretation of experimental order parameters using MD simulations in previous sections suggest that PC, PE, PG and PS lipid headgroups are very flexible, allowing them to bind proteins in various different conformations. To test this prediction, we analyzed the conformations of all protein-bound lipids from structures deposited in the PDB [5]. We found 311 PC, 394 PE, 154 PG, and 35 PS lipid conformations that were bound to different types of proteins (including both integral and peripheral membrane proteins) and were determined as a part of protein structure using crystallography or cryo-EM. The full list of structures with bound lipids is available from *Data/PDBdistributions/pdbtable.pdf* in Ref. [41].

The heavy atom dihedral angle distributions calculated from these conformations (Fig. 4 A) reveal that the protein-bound lipids indeed exhibit wide range of conformations independently on the headgroup type. As for bulk lipid bilayers, only *cis* conformations of P-O_α-C_α-C_β and g_2-g_3-O_{g3}-P dihedrals are almost completely absent in all lipids, and significant differences between different headgroups were not observed. Structures deviating from lipid crystals have been previously proposed to indicate inaccuracies in lipid structures in PDB [8, 15]. However, we observe large deviations from lipid crystals structures also in conformational ensembles that reproduce the NMR data in the liquid lamellar phase, indicating that such deviations are realistic also in protein-bound states.

Our results suggest that flexible lipid headgroups can optimize the intermolecular interactions with proteins by binding in a wide range of conformations. Therefore, the specific

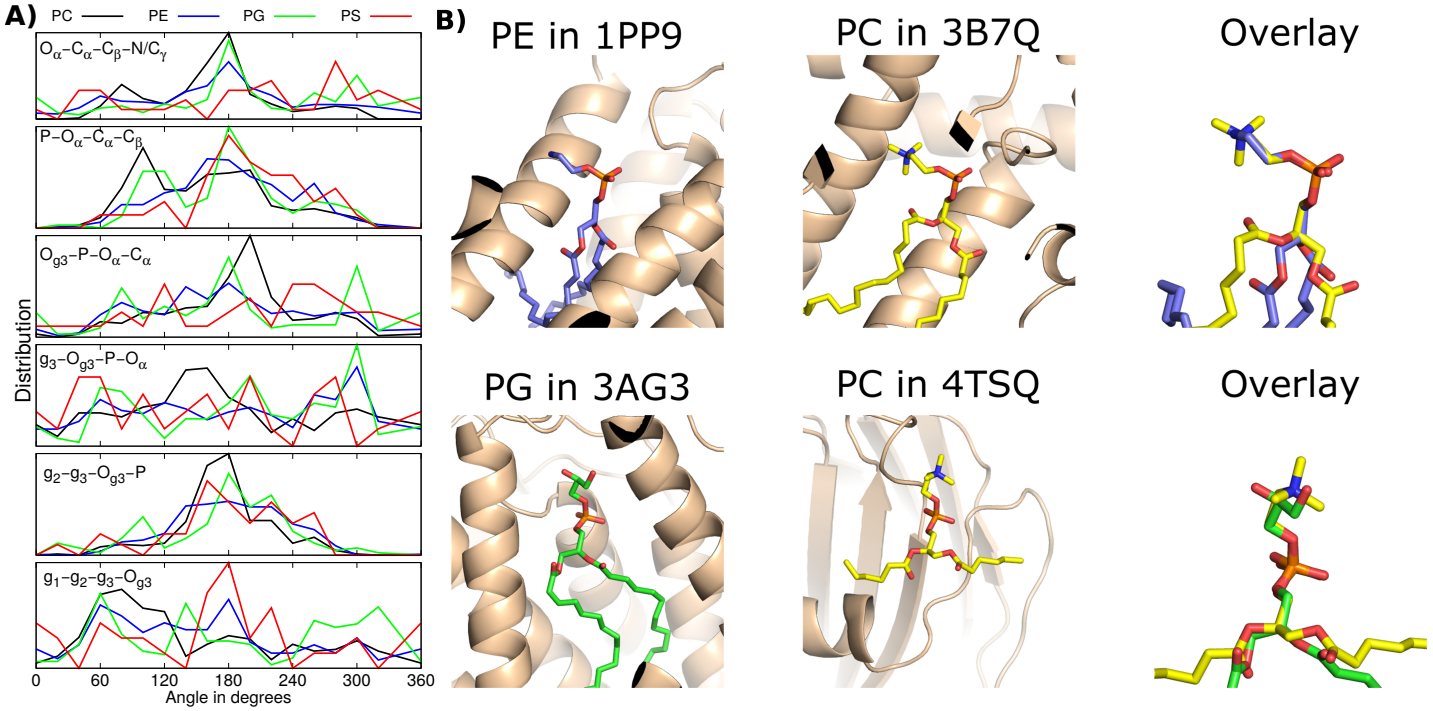

FIG. 4: A) Heavy atom dihedral angle distributions calculated from lipid structures in PDB. B) The structure of PE headgroup bound to cytochrome bc_1 complex (PDB ID: 1PP9 [46]) with identical conformation as the PC headgroup bound to yeast Sec14 (PDB ID: 3B7Q [47]), and the structure of PG headgroup bound to bovine cytochrome *c* oxidase (PDB ID: 3AG3 [48]) with identical conformation as PC to FraC, a pore-forming toxin (PDB ID: 4TSQ [49]).

binding of lipids to proteins is not driven by the structural differences between headgroups. This is demonstrated in Fig. 4 B with two examples where different lipids bound to different proteins have almost identical headgroup conformations: PE in cytochrome bc_1 complex is similar to PC bound to yeast Sec14, and PG bound to bovine cytochrome *c* oxidase is similar to PC bound to pore-forming toxin (FraC). On the other hand, a single lipid headgroup type is capable of accommodating various binding positions and as such would be able to specifically bind to many different kinds of binding sites in different proteins.

CONCLUSIONS

C–H bond order parameters from NMR experiments suggest that lipid headgroup conformational ensembles depend on lipid type (PC, PE, PG or PS) and accumulated membrane charge (cationic lipids, surfactants, ions or drugs). Our interpretation of these data, using MD simulations collected within the NMRlipids open collaboration, revealed that the differences in order parameters can be explained by relatively small changes in dihedral angle probability distributions. All studied headgroups (PC, PE, PG and PS) are flexible and access a similar wide range of conformations with only very few restictions in dihedral orientations also when charges are bound to membranes. The observed differences in order parameters originate from reweighting conformational probabilities rather than changes in accessible structures.

The flexibility and wide conformational space of headgroups suggest that protein–bound lipids can adapt to various binding sites to optimize the intermolecular lipid–protein interactions. We tested this prediction by analyzing the conformations of lipids that are tightly bound to proteins in the PDB. Indeed, also protein–bound lipids exhibit wide range of conformations without significant differences between different lipid types. Therefore, the specificify of lipid binding to proteins is not regulated by accessible structures of lipids, and a single lipid type can adapt to various binding sites in proteins.

Our results pave the way toward the understanding of lipid-mediated cell signaling and how lipids regulate membrane protein function in general. We suggest that the key to understand selective binding of certain lipid types to proteins are intermolecular lipid–protein interactions, rather than conformational restrictions of the lipids. On the other hand, broad conformational ensembles in bulk bilayers suggest that lipid crystal structures play a minor role while the entropic cost of lipid binding may be significant. Finally, we demonstrated the power of open access MD simulation data from the NMRlipids open collaboration to complement the data in the PDB for elucidating how complex systems made up of disordered biomolecules behave.

AP is grateful to the Centro de Supercomputacin de Galicia

(CESGA) for use of the Finis Terrae computer MJ thanks CSC – IT Center for Science for computational resources and the Emil Aaltonen foundation for financial support.

P.B. was supportedby the Academy of Finland (Grant 311031)

F.F.-R. acknowledges Tecnológico Nacional de México Proyecto IT16C431, Dirección General de Asuntos del Personal Académico (DGAPA) Programa de Apoyo a Proyectos de Investigación e Innovación Tecnológica (PAPIIT) IG100920, CONACyT Ciencia de Frontera 74884 for financial support and Miztli-Dirección de Cómputo y de Tecnologías de Información y Comunicación (DGTIC) - Universidad Nacional Autónoma de México (UNAM) (Project LANCAD-UNAM-DGTIC-057) facilities for computing-time allocation.

I.G. was supported by the Ministry of Science and Higher Education of the Russian Federation (agreement #075-00337-20-03, project FSMG-2020-0003).

J.J.M. gratefully acknowledges financial support from the Carlsberg Foundation in the form of a postdoctoral fellowship while at the University of Chicago (grants CF15-0552, CF16-0639, and CF17-0783) and the research framework provided by the Research Computing Center at the University of Chicago.

O.H.S.O, A.M.K, and S.I.V acknowledge CSC – IT Center for Science for computational resources and Academy of Finland (315596 and 319902) for financial support.

T.J.P acknowledges use of the Iridis high-performance computing resources at the University of Southampton.

* samuli.ollila@helsinki.fi

[1] A. Lee, Biochimica et Biophysica Acta (BBA) - Biomembranes **1612**, 1 (2003), ISSN 0005-2736, URL http://www.sciencedirect.com/science/article/pii/S0005273603000567.

[2] G. van Meer, D. R. Voelker, and G. W. Feigenson, Nature Reviews Molecular Cell Biology **9**, 112 (2008), URL https://doi.org/10.1038/nrm2330.

[3] M. A. Lemmon, Nat. Rev. Mol. Cell Biol. **9**, 99 (2008).

[4] A. G. Lee, Trends in Biochemical Sciences **36**, 493 (2011), URL https://doi.org/10.1016/j.tibs.2011.06.007.

[5] H. M. Berman, J. Westbrook, Z. Feng, G. Gilliland, T. N. Bhat, H. Weissig, I. N. Shindyalov, and P. E. Bourne, Nucleic Acids Research **28**, 235 (2000), ISSN 0305-1048, https://academic.oup.com/nar/article-pdf/28/1/235/9895144/280235.pdf, URL https://doi.org/10.1093/nar/28.1.235.

[6] G. Büldt and R. Wohlgemuth, The Journal of Membrane Biology **58**, 81 (1981), ISSN 1432-1424, URL http://dx.doi.org/10.1007/BF01870972.

[7] I. Pascher, M. Lundmark, P.-G. Nyholm, and S. Sundell, Biochim. Biophys. Acta **1113**, 339 (1992).

[8] D. Marsh and T. Páli, European Biophysics Journal **42**, 119 (2013), URL https://doi.org/10.1007/s00249-012-0816-6.

[9] J. Seelig, Q. Rev. Biophys. **10**, 353 (1977).

[10] J. H. Davis, Biochim. Biophys. Acta **737**, 117 (1983).

[11] D. J. Semchyschyn and P. M. Macdonald, Magn. Res. Chem. **42**, 89 (2004).

[12] H. U. Gally, G. Pluschke, P. Overath, and J. Seelig, Biochemistry **20**, 1826 (1981).

[13] R. Wohlgemuth, N. Waespe-Sarcevic, and J. Seelig, Biochemistry **19**, 3315 (1980).

[14] O. S. Ollila and G. Pabst, Biochim. Biophys. Acta **1858**, 2512 (2016).

[15] W. Pezeshkian, H. Khandelia, and D. Marsh, Biophysical Journal **114**, 1895 (2018), ISSN 0006-3495, URL http://www.sciencedirect.com/science/article/pii/S0006349518302467.

[16] H. Akutsu, Biochimica et Biophysica Acta (BBA) - Biomembranes **1862**, 183352 (2020), URL https://doi.org/10.1016/j.bbamem.2020.183352.

[17] C. Sohlenkamp and O. Geiger, FEMS Microbiology Reviews **40**, 133 (2015).

[18] J. E. Vance, Traffic **16**, 1 (2015).

[19] E. Calzada, O. Onguka, and S. M. Claypool (Academic Press, 2016), vol. 321 of *International Review of Cell and Molecular Biology*, pp. 29 – 88.

[20] D. Patel and S. N. Witt, Oxidative Medicine and Cellular Longevity **2017**, 4829180 (2017).

[21] P. A. Leventis and S. Grinstein, Annual Review of Biophysics **39**, 407 (2010).

[22] P. Hariharan, E. Tikhonova, J. Medeiros-Silva, A. Jeucken, M. V. Bogdanov, W. Dowhan, J. F. Brouwers, M. Weingarth, and L. Guan, BMC Biology **16**, 85 (2018).

[23] P. L. Yeagle, Biochimica et Biophysica Acta (BBA) - Biomembranes **1838**, 1548 (2014), membrane Structure and Function: Relevance in the Cell's Physiology, Pathology and Therapy.

[24] P. Scherer and J. Seelig, EMBO J. **6** (1987).

[25] J. Seelig, Cell Biology International Reports **14**, 353 (1990), ISSN 0309-1651, URL http://www.sciencedirect.com/science/article/pii/030916519091204H.

[26] F. Vigant, N. C. Santos, and B. Lee, Nature Reviews Microbiology **13**, 426 (2015).

[27] T. M. Ferreira, F. Coreta-Gomes, O. H. S. Ollila, M. J. Moreno, W. L. C. Vaz, and D. Topgaard, Phys. Chem. Chem. Phys. **15**, 1976 (2013).

[28] T. M. Ferreira, R. Sood, R. Bärenwald, G. Carlström, D. Topgaard, K. Saalwächter, P. K. J. Kinnunen, and O. H. S. Ollila, Langmuir **32**, 6524 (2016).

[29] S. V. Dvinskikh, H. Zimmermann, A. Maliniak, and D. Sandstrom, J. Magn. Reson. **168**, 194 (2004).

[30] J. D. Gross, D. E. Warschawski, and R. G. Griffin, J. Am. Chem. Soc. **119**, 796 (1997).

[31] M. Bak, J. T. Rasmussen, and N. C. Nielsen, Journal of Magnetic Resonance **147**, 296 (2000), ISSN 1090-7807, URL http://www.sciencedirect.com/science/article/pii/S1090780700921797.

[32] H. Antila, P. Buslaev, F. Favela-Rosales, T. M. Ferreira, I. Gushchin, M. Javanainen, B. Kav, J. J. Madsen, J. Melcr, M. S. Miettinen, et al., J. Phys. Chem. B **123**, 9066 (2019).

[33] D. Marsh, *Handbook of Lipid Bilayers, Second Edition* (RSC press, 2013).

[34] A. Botan, F. Favela-Rosales, P. F. J. Fuchs, M. Javanainen, M. Kanduč, W. Kulig, A. Lamberg, C. Loison, A. Lyubartsev, M. S. Miettinen, et al., J. Phys. Chem. B **119**, 15075 (2015).

[35] A. Catte, M. Girych, M. Javanainen, C. Loison, J. Melcr, M. S. Miettinen, L. Monticelli, J. Maatta, V. S. Oganesyan, O. H. S. Ollila, et al., Phys. Chem. Chem. Phys. **18**, 32560 (2016).

[36] F. Borle and J. Seelig, Chem. Phys. Lipids **36**, 263 (1985).
[37] J. Seelig and H. U. Gally, Biochemistry **15**, 5199 (1976).
[38] H. M. Berman, J. Westbrook, Z. Feng, G. Gilliland, T. N. Bhat, H. Weissig, I. N. Shindyalov, and P. E. Bourne, Nucleic Acids Research **28**, 235 (2000), ISSN 0305-1048.
[39] N. Michaud-Agrawal, E. J. Denning, T. B. Woolf, and O. Beckstein, J. Comput. Chem. **32**, 2319 (2011), https://onlinelibrary.wiley.com/doi/pdf/10.1002/jcc.21787, URL https://onlinelibrary.wiley.com/doi/abs/10.1002/jcc.21787.
[40] Richard J. Gowers, Max Linke, Jonathan Barnoud, Tyler J. E. Reddy, Manuel N. Melo, Sean L. Seyler, Jan Domaski, David L. Dotson, Sbastien Buchoux, Ian M. Kenney, et al., in *Proceedings of the 15th Python in Science Conference*, edited by Sebastian Benthall and Scott Rostrup (2016), pp. 98 – 105.
[41] N. project, *Nmrlipidsivb github repository*, URL https://github.com/NMRLipids/NMRlipidsIVPEandPG.
[42] P. G. Scherer and J. Seelig, Biochemistry **28**, 7720 (1989).
[43] J. L. Browning and J. Seelig, Biochemistry **19**, 1262 (1980).
[44] J. Seelig, P. M. MacDonald, and P. G. Scherer, Biochemistry **26**, 7535 (1987).
[45] J. Melcr, T. M. Ferreira, P. Jungwirth, and O. H. S. Ollila, J. Chem. Theo. Comput. **16**, 738 (2020).
[46] L. shar Huang, D. Cobessi, E. Y. Tung, and E. A. Berry, Journal of Molecular Biology **351**, 573 (2005), ISSN 0022-2836, URL https://www.sciencedirect.com/science/article/pii/S0022283605006078.
[47] G. Schaaf, E. A. Ortlund, K. R. Tyeryar, C. J. Mousley, K. E. Ile, T. A. Garrett, J. Ren, M. J. Woolls, C. R. Raetz, M. R. Redinbo, et al., Molecular Cell **29**, 191 (2008), ISSN 1097-2765, URL https://doi.org/10.1016/j.molcel.2007.11.026.
[48] K. Muramoto, K. Ohta, K. Shinzawa-Itoh, K. Kanda, M. Taniguchi, H. Nabekura, E. Yamashita, T. Tsukihara, and S. Yoshikawa, Proceedings of the National Academy of Sciences **107**, 7740 (2010), ISSN 0027-8424, https://www.pnas.org/content/107/17/7740.full.pdf, URL https://www.pnas.org/content/107/17/7740.
[49] K. Tanaka, J. M. Caaveiro, K. Morante, J. M. González-Mañas, and K. Tsumoto, Nature Communications **6**, 6337 (2015), ISSN 2041-1723, URL https://doi.org/10.1038/ncomms7337.

ToDo